

Antagonistic Functions of Dishevelleds Regulate Frizzled3 Endocytosis via Filopodia Tips in Wnt-Mediated Growth Cone Guidance

Keisuke Onishi,¹ Beth Shafer,¹ Charles Lo,¹ Fadel Tissir,² Andre M. Goffinet,² and Yimin Zou¹

¹Neurobiology Section, Biological Sciences Division University of California, San Diego, La Jolla, California 92093 and ²Université Catholique de Louvain, Institute of Neuroscience, Brussels, B-1348 Belgium

How growth cones detect small concentration differences of guidance cues for correct steering remains a long-standing puzzle. Commissural axons engage planar cell polarity (PCP) signaling components to turn anteriorly in a Wnt gradient after midline crossing. We found here that Frizzled3, a Wnt receptor, undergoes endocytosis via filopodia tips. Wnt5a increases Frizzled3 endocytosis, which correlates with filopodia elongation. We discovered an unexpected antagonism between Dishevelleds, which may function as a signal amplification mechanism in filopodia where PCP signaling is activated: Dishevelled2 blocks Dishevelled1-induced Frizzled3 hyperphosphorylation and membrane accumulation. A key component of apical-basal polarity (A-BP) signaling, aPKC, also inhibits Dishevelled1-induced Frizzled3 hyperphosphorylation. *Celsr3*, another PCP component, is required in commissural neurons for anterior turning. Frizzled3 hyperphosphorylation is increased in *Celsr3* mutant mice, where PCP signaling is impaired, suggesting Frizzled3 hyperphosphorylation does correlate with loss of PCP signaling *in vivo*. Furthermore, we found that the small GTPase, Arf6, which is required for Frizzled3 endocytosis, is essential for Wnt-promoted outgrowth, highlighting the importance of Frizzled3 recycling in PCP signaling in growth cone guidance. In a Wnt5a gradient, more Frizzled3 endocytosis and activation of atypical protein kinase C was observed on the side of growth cones facing higher Wnt5a concentration, suggesting that spatially controlled Frizzled3 endocytosis is part of the key mechanism for growth cone steering.

Introduction

In stark contrast to our rich knowledge on the molecular identity of axon guidance cues, the logic of growth cone signaling leading to directionality remains fragmentary (Bashaw and Klein, 2010). Wnt-Frizzled signaling is essential for anterior turning of spinal cord commissural axons after midline crossing and is an excellent model for studying growth cone steering mechanisms (Lyuksytova et al., 2003). Members of apical-basal polarity (A-BP) and planar cell polarity (PCP) signaling, atypical protein kinase C (aPKC), Frizzled3, Vangl2, Celsr3, and Dishevelled1, have been shown to be required in mediating Wnt attraction and anterior turning (Wolf et al., 2008; Shafer et al., 2011), suggesting that cell polarity signaling pathways play a central role in polarizing growth cones right after midline crossing. How PCP and A-BP

signaling pathways function to steer growth cones is not well understood.

We found the Wnt-binding receptor Frizzled3 undergoes endocytosis via the tips of growth cone filopodia. Wnt5a promotes endocytosis of Frizzled3, which is mediated by Arf6, a small GTPase, to stimulate Wnt-stimulated outgrowth. We uncovered a novel difference among the three Dishevelleds. While Dishevelled1 induces Frizzled3 hyperphosphorylation and membrane accumulation, Dishevelled2 does not; instead, Dishevelled2 prevents Dishevelled1 from inducing Frizzled3 hyperphosphorylation. The activation of Dishevelled2 may cause the release of inhibition Dishevelled1 has on Frizzled3 endocytosis to allow for amplification of PCP signaling in a select set of filopodia. Consistent with these results, in a Wnt5a gradient, more Frizzled3 endocytosis and activation of aPKC were observed on the side facing higher Wnt5a concentration. We propose that the integrated functions of PCP and A-BP signaling pathways endow the growth cones with high sensitivity for guidance cues to control the direction of turning.

Materials and Methods

Plasmids, reagents, and antibodies. Mouse Frizzled3 was subcloned into C-terminal tdTomato tag expression vectors (modified pCAGEN). FLAG sequences were inserted between 24 and 25 aa in the N terminal (following the predicted signal peptide sequences; 1–22) of mouse Frizzled3. Frizzled3-HA, Dishevelled1-FLAG, Dishevelled1-EGFP, and Dishevelled2-FLAG expressing constructs are described previously

Received July 1, 2013; revised Sept. 2, 2013; accepted Sept. 28, 2013.

Author contributions: Y.Z. designed research; K.O. performed research; B.S., C.L., F.T., and A.M.G. contributed unpublished reagents/analytic tools; K.O. and Y.Z. analyzed data; K.O. and Y.Z. wrote the paper.

This work was supported by a National Institutes of Health (NIH) RO1 (NS047484) to Y.Z., a postdoctoral Fellowship from Japan Society for Promotion of Sciences to K.O., a postdoctoral Fellowship from Spinal Cord Research Foundation of Paralyzed Veterans of America to C.L., and a postdoctoral Fellowship from NIH/National Institute of Neurological Disorders and Stroke training grant (T32 NS007220–27) to C.L. We thank Jim Casanova for his generous gifts of the Arf6 wild-type and mutant constructs and Sourav Ghosh for Par6 constructs. We thank Zou lab members Edmund Hollis II, Anna Tury, Sonal Thakar, Virginia Hazen, Liqing Wang, John Scott, and Alex Goetz for critical reading of this manuscript and helpful comments.

Correspondence should be addressed to Yimin Zou, Neurobiology Section, Biological Sciences Division, University of California, San Diego, La Jolla, CA 92093. E-mail: yzou@ucsd.edu.

DOI:10.1523/JNEUROSCI.2800-13.2013

Copyright © 2013 the authors 0270-6474/13/3319071-15\$15.00/0

(Shafer et al., 2011). Dishevelled3 was amplified from mouse E16.5 brain cDNA library and subcloned into C-terminal FLAG tag expression vector (pZou-FLAG). aPKC constructs were described previously (Wolf et al., 2008). PAR6 expression vector was kindly provided by Dr. Sourav Ghosh. Hemagglutinin (HA)-tagged Arf6 WT, T27N, T157, and EGFP-Rab11 constructs were kindly given by Dr. James E. Casanova. EGFP-Rab4, 5, and 8 constructs were a kind gift from Dr. Johan Peranen. To make EGFP-tagged Arf6 series, Arf6 WT, T27N, and T157 were amplified by PCR from HA-tagged Arf6 series and subcloned into pEGFP-N2.1 (β -actin promoter; modified from pEGFP-N2; Clontech). All constructs were verified by sequencing (Eton Biosciences).

Sequences of the shRNA constructs are as follows: control shRNA (5'-GA AACGAAAGCAGGTACG-3'), human Dishevelled1 shRNA (5'-CAGT CTGAAAGTACGTGGA-3'), human Dishevelled2 shRNA (5'-TG TGACCTCCTCCTCCAGT-3'). Complementary oligonucleotides were annealed and inserted into pSuper-retro-neo-GFP. The plasmid encoding shRNA against rat Arf6 (target sequence; 5'-CCTCATCTTCGCCAACAA GCAGGACCTGC-3') and control shRNA plasmid (TR30008) were purchased from Origene (pGFP-V-RS vector). All constructs were verified by sequencing (Eton Bioscience).

Recombinant Wnt5a was purchased from R&D Systems, and Sulfo-NHS-LC-Biotin and NeutrAvidin agarose were from Pierce. The primary antibodies used in this study include anti-Frizzled3 (R&D Systems), anti- α -Adaptin (BD Transduction Laboratories), anti-Amphiphysin (BD Transduction Laboratories), anti-AP180 (BD Transduction Laboratories), anti-FLAG (M2; Sigma), anti-HA (Covance), anti-GFP (Abcam), anti-PKC ζ (Santa Cruz Biotechnology), anti-pPKC ζ (T410; Santa Cruz Biotechnology), anti-Rac1 (BD Transduction Laboratories), anti-phospho-c-Jun (Ser63; Cell Signaling Technology), anti-c-Jun (Cell Signaling Technology), anti-phospho-JNK (Thr183/Tyr185; Cell Signaling Technology), anti-JNK (Cell Signaling Technology), anti-Dishevelled1 (Santa Cruz Biotechnology), anti-Dishevelled2 (Cell Signaling Technology), anti-GAPDH (Millipore), anti-Insulin Receptor β (Santa Cruz Biotechnology), anti-TAG-1 (Developmental Studies Hybridoma Bank), and anti-L1 (Developmental Studies Hybridoma Bank). Anti-Frizzled3 antibodies for immunoblotting were kindly provided by Dr. Yanshu Wang and Dr. Jeremy Nathans (Wang et al., 2006). Alexa Fluor-conjugated secondary antibodies for mouse/rabbit/rat IgG and mouse IgM were purchased from Invitrogen. Horseradish peroxidase-conjugated secondary antibodies for mouse/rabbit/goat IgG were purchased from Jackson ImmunoResearch. Anti-Celsr3 rabbit polyclonal antibodies were generated in the Zou lab (Fenstermaker et al., 2010).

Commissural neuron culture and time-lapse imaging. Rat E13 and mouse E11.5 embryos of either sex were dissected and commissural neuron culture was prepared as previously described (Wolf et al., 2008; Shafer et al., 2011). Dissociated commissural neurons were plated in a 35 mm glass-bottom dish (MatTek) coated with 20 μ g/ml PDL for time-lapse imaging or 24-well dish coated with PDL for immunocytochemistry. Electroporations of rat E13 spinal cords were performed as described previously (Wolf et al., 2008). Time-lapse imaging was performed using Olympus IX81 inverted microscope and PerkinElmer UltraView Vox Spinning Disk Confocal system (Shafer et al., 2011). Images of the growth cones were obtained every 3 s for 5 min. Before taking images, neurons were incubated with Alexa Fluor 488-conjugated anti-FLAG antibodies for 15 min and then washed to remove unbound anti-FLAG antibodies. Subsequently neurons were treated with Wnt5a (100 ng/ml) to analyze the effects on the direction of Frizzled3 vesicle movement. Frizzled3-tdTomato vesicles are tracked manually in 14 growth cones, 48 filopodia, 298 vesicles for WT, 11 growth cones, 37 filopodia, 213 vesicles for WT with Wnt5a, 9 growth cones, 21 filopodia, 101 vesicles for 7A, 5 growth cones, 20 filopodia, and 78 vesicles for 7A with Wnt5a. Images were acquired using Volocity software (PerkinElmer). To investigate Arf6-EGFP movement, a total of 41 growing filopodia and 28 shrinking filopodia from six growth cones were analyzed and quantified.

Measurement of FLAG-Frizzled3-tdTomato intensity. To quantify the Frizzled3 cell-surface amount in commissural neurons, rat commissural neurons expressing FLAG-Frizzled3 WT or 7A-tdTomato were incubated with Alexa Fluor 488-conjugated anti-FLAG antibodies for 15 min. After washing out unbound anti-FLAG antibodies, neurons were fixed with 4% paraformaldehyde (PFA) for 15 min at 37°C, washed again, and

then immediately mounted. Images were taken using a Zeiss LSM 510 confocal microscope, and analyzed using ImageJ software. Fifteen growth cones for each condition from three independent experiments were analyzed.

Quantification of Frizzled3 colocalization with AP-2 at the tips of filopodia. Commissural neuron cultures were treated with or without 100 ng/ml Wnt5a for 5 min, followed by 4% PFA fixation for 15 min at 37°C. Cells were then immunostained with anti-Frizzled3 (R&D Systems) and anti- α -Adaptin (BD Transduction Laboratories). Growth cone images were taken by using Zeiss LSM510, and colocalization was quantified manually.

Wnt5a gradient in Dunn chamber. For Dunn chamber assays, primary commissural neurons were grown on appropriately coated 18 mm square coverslips (Fisher Scientific) at a low density such that individual isolated neurons were present (150,000 cells/well in a 6-well plate for commissural neurons). The Dunn chamber assembly protocol was described previously (Yam et al., 2009). The Dunn chambers were prewashed twice with conditioned media. Conditioned media was added to fill the inner and outer wells. A coverslip with neurons was inverted over the Dunn chamber, leaving a narrow slit at the edge for draining and refilling the outer well. Excess media was removed by paper, and three sides of the Dunn chamber were sealed with hot paraffin:vaseline. Using a piece of paper towel, all the liquid from the outer well was removed through the filling slit, and the Wnt5a (100 ng/ml; diluted in conditioned media) was added to the outer well by using a 1 cc insulin syringe. The filling slit was then sealed with hot paraffin:vaseline. Dunn chambers were assembled rapidly (<5 min) to avoid changes in the pH of the media. After assembly, the Dunn chamber was put back into 37°C CO₂ incubator for 30 min. Then the coverslip was immediately removed from the Dunn chamber and put into 4% PFA solution for 15 min at 37°C for fixation followed by immunostaining.

To quantify Fzd3/AP-2 colocalization and p-aPKC localization, only the growth cones that direct perpendicularly to the Wnt5a gradient were analyzed. The line was drawn at the middle of the growth cone and then Fzd3 and AP-2 colocalization in the proximal side and distal side were counted manually. Using ImageJ, p-PKC ζ intensity was measured and divided by the area of proximal or distal side to normalize. Then P/D ratio was calculated. For Fzd3/AP-2 colocalization, we analyzed 38 growth cones (bovine serum albumin (BSA) control) and 39 growth cones (Wnt5a) from four independent experiments. For p-PKC ζ intensity, we analyzed 29 growth cones (BSA control) and 29 growth cones (Wnt5a gradient) from three independent experiments.

Glutathione S-transferase-pull-down assay, surface biotinylation, avidin precipitation, Rac activation assay, immunoprecipitation, phosphatase/glycosidase assay, and biochemical analyses. Glutathione S-transferase (GST) or GST fusion of the cytoplasmic region of Frizzled3 (GST-Fzd3cyto; 505–666 aa) were generated using pGEX4T-1. All GST fusions were expressed in BL21 *Escherichia coli* and purified with glutathione-Sepharose 4B (GSH beads; GE Healthcare). The whole-brain lysates were prepared from WT mouse P14 brains. P14 brains were homogenized and lysed with pull-down buffer (20 mM Tris HCl, pH 7.4, 150 mM NaCl, 1 mM EDTA, 1 mM EGTA, 5 mM NaF, 10 mM β -glycerophosphate, 1 mM Na₃VO₄, 1 mM dithiothreitol, and protease inhibitor cocktail and 0.5% TX-100). GST fusion proteins (20 mg) immobilized with GSH beads were combined with whole-brain extract (~1 mg) in the pull-down buffer. After incubation for 1 h on a rotating wheel at 4°C, beads were separated from the supernatant by centrifugation and washed three times in the TBS-T (0.1% Tween 20), and the proteins retained on the beads (not including the GST fusions) were analyzed by Western blotting.

Cell-surface biotinylation and avidin precipitation were performed as described previously (Shafer et al., 2011). After 24 h of transfection (FuGENE6; Roche), cell-surface proteins were labeled with 1 mg/ml Sulfo-NHS-LC-Biotin on ice for 45 min. After quenching active biotin by glycine, the cell lysates were incubated with NeutrAvidin agarose for 1 h and then precipitated. The total extract and avidin-bound fraction were analyzed by Western blotting. To do phosphatase and glycosidase assay, avidin-bound fractions were treated with BSA or alkaline phosphatase (Roche) for 60 min at 37°C. Then the samples were boiled with denaturing solution (NEB) and treated with BSA or PNGase F (NEB) for

60 min at 37°C. Samples were then boiled again and subjected to immunoblotting.

Activation of Rac1 was assayed using GST-CRIB. After HEK293 cells were incubated in serum-free DMEM for 24 h, the cells were stimulated with 100 ng/ml Wnt5a for the indicated time. Cells were lysed in 500 μ l Rac pull-down buffer (20 mM Tris-HCl, pH 7.4, 150 mM NaCl, 10 mM MgCl₂, 1% NP-40, 10% glycerol, and protease inhibitor). Lysates were incubated with GST-CRIB immobilized glutathione-Sepharose (20 μ g GST-CRIB/10 μ l GSH-Sepharose) for 1 h at 4°C. Glutathione-Sepharose was precipitated by centrifugation, washed with TBS-T (0.05% Tween 20) three times, boiled, and then analyzed by Western blotting. For immunoprecipitation assay, cell lysates were incubated with the indicated antibodies for 1 h at 4°C, then protein A/G plus agarose (Santa Cruz Biotechnology) was added and rotated for 1 h at 4°C. Agarose was precipitated by centrifugation, washed with TBS-T (0.05% Tween 20) three times, boiled, and then analyzed by Western blotting.

All biochemical experiments in figures were performed at least three times and all images are representatives.

Mouse lines. *Celsr3* mutant and floxed mice were generated by Dr Andre Goffinet. *Wnt1-Cre* transgenic mice were purchased from The Jackson Laboratory. To produce *Wnt1-Cre* driven *Celsr3* conditional knock-out mice, *Wnt1-Cre* transgenic mice were mated with heterozygous mice carrying the *Celsr3*^{lox} allele. Subsequently they were mated with mice homozygous for the *Celsr3*^{lox} allele (*Celsr3*^{lox/lox}) to obtain embryos of either sex with *Celsr3*^{lox/flox}; *Wnt1-Cre* genotype. Genotyping of all animals was done by PCR using genomic DNA prepared from tails. Experiments were conducted in accordance with the National Institutes of Health Guide for the Care and Use of Laboratory Animals and approved by the University of California San Diego Animal Subjects Committee.

Immunohistochemistry. E11.5 mouse embryos were fixed in 4% PFA for 2 h on ice. After equilibration with 30% (w/v) sucrose in PBS, the fixed embryos were embedded in OCT compound (Sakura) and frozen. Transverse sections were prepared by cutting frozen brain with a cryostat (CM3050S; Leica) at a thickness of 20 μ m and mount on a glass slides (SuperFrost Plus; Fisher Scientific). Slides were washed in TBS-T (0.1% Tween 20), then incubated in 2% donkey serum in TBS-T (blocking solution) for 30 min at room temperature. Slides were further incubated with primary antibodies diluted in blocking solution for overnight at 4°C. The slides were washed three times for 10 min each in TBS-T, and then incubated for 1 h with secondary antibodies diluted in blocking solution at room temperature, washed again, and mounted using Fluoromount G (Southern Biotech). Images were taken using a Zeiss LSM 510 confocal microscope.

Open-book preparation and DiI axon labeling. Mouse E11.5 spinal cord open-books were prepared as described previously (Zou et al., 2000; Lyuksyutova et al., 2003; Shafer et al., 2011). Mouse spinal cord open-books were immediately fixed with 4% PFA. To visualize anterior-posterior projection of commissural axon, DiI labeling was used in the open-book preparation. DiI injection and quantification were completed as described previously (Zou et al., 2000; Lyuksyutova et al., 2003; Wolf et al., 2008; Shafer et al., 2011). The number of injection sites and embryos are indicated in Figure 5D.

Statistical analysis. Statistical analysis for multiple comparison was performed using one-way ANOVA followed by a Bonferroni *post hoc* test for multiple comparisons. To compare two groups, Student's *t* test was used (two-tailed distribution). To compare Frizzled3/AP-2 colocalization or filopodia number between in the proximal and distal side (see Fig. 8C,D), we used Wilcoxon signed-rank test. We used one-way ANOVA followed by Bonferroni *post hoc* test when we compared colocalization or filopodia number between BSA in the proximal and Wnt5a proximal side (or between BSA distal and Wnt5a distal side).

Results

Frizzled3 is colocalized with AP-2 complexes at the tip of filopodia in commissural axon growth cones

Clathrin and AP-2-mediated endocytosis of Frizzled3 is a critical step for PCP signaling (Yu et al., 2007; Sato et al., 2010). We

previously proposed that Vangl2, which is enriched on the tips of growing filopodia, promotes Frizzled3 endocytosis (Shafer et al., 2011). Here, we directly tested whether Frizzled3 can be endocytosed at the tip of filopodia in the growth cones. WT mouse E11.5 embryos were dissected and dorsal spinal commissural neurons were dissociated and cultured for 2 d. Commissural neurons were then stimulated with Wnt5a and stained with anti-Frizzled3 antibodies and anti- α -Adaptin antibodies to detect endogenous Frizzled3 and AP-2 complex (Fig. 1A). We found that endogenous AP-2 complexes can be observed at the tip of filopodia. Moreover, Wnt5a enhanced Frizzled3 colocalization with AP-2 at filopodia tips (Fig. 1A,B). Wnt5a treatment did not change total filopodia number during the time frame of our observation (5 min; Fig. 1C). We also tested whether Frizzled3 can interact with other components of endocytic machinery. We prepared GST-fused mouse Frizzled3 cytoplasmic tail (GST-Fzd3cyto; 505–666 aa; Fig. 1D) and performed GST-pull-down assay using mouse P14 whole-brain extract. α -Adaptin was precipitated with GST-Fzd3cyto but not GST protein only (Fig. 1D). This is consistent with Frizzled3 being colocalized with α -Adaptin. Moreover, AP180 and Amphiphysin, which bind to AP-2 and regulate clathrin and AP-2-mediated endocytosis, were also precipitated with GST-Fzd3cyto. Because we used the C-terminal domain of Frizzled3, which does not include Dishevelled binding region, our results suggest that Frizzled3 interacts with endocytic machinery directly rather than through Dishevelleds (Fig. 1E). Furthermore, we found that 5 min of Wnt5a treatment did not affect EphB1 and AP-2 colocalization at the tip of filopodia (Fig. 1F,G). This result suggests that Wnt5a effect is specific to Frizzled3. Together, these results suggest that Frizzled3 can be endocytosed at the tips of filopodia and Wnt5a promotes Frizzled3 endocytosis at the tips.

Frizzled3 undergoes endocytosis via the tips of filopodia

We then tracked Frizzled3 using a double-labeling construct (Fig. 2A). Frizzled3 was tagged with tdTomato to the carboxyl domain and the FLAG epitope tag was engineered to the extracellular N terminus. First, we tested whether this Flag-Frizzled3-tdTomato can still transduce Wnt-PCP signaling. We found that in HEK293 cells expressing Flag-Frizzled3-tdTomato, Wnt5a increased the level of phosphorylated c-Jun, suggesting that Flag-Frizzled3-tdTomato are functional (Fig. 2B). Plasma membrane-localized Frizzled3 was pulse labeled by anti-FLAG antibodies conjugated with Alexa Fluor 488. We then performed time-lapse imaging in the commissural axonal growth cones using Spinning Disk Confocal microscopy (Fig. 2E–G). The yellow Frizzled3 vesicles represent the cell-surface Frizzled3 when the cells were pulse labeled with anti-FLAG antibodies. The red Frizzled3 vesicles are nascent Frizzled3 pools, which were not on the cell surface when the anti-FLAG antibodies were added briefly.

We found that yellow Frizzled3 vesicles continuously emerged from the tips of growth cone filopodia and they moved inward along the filopodia (Fig. 2F,G, Row 1–4). These new yellow vesicles contain the FLAG antibody labeled Frizzled3 protein newly endocytosed. Some of the vesicles moved all the way into the central domain of the growth cone. Some yellow Frizzled3 vesicles were transported out to the tip of filopodia and then disappeared. It is likely that these vesicles exocytosed on the tips and then the fusion protein immediately diffused in the plasma membrane (Fig. 2F,G, Row 1–4; dash-line boxes indicate the position of high-magnification images). We also made a similar construct using a mutant Frizzled3 (7A) with all seven phosphorylation

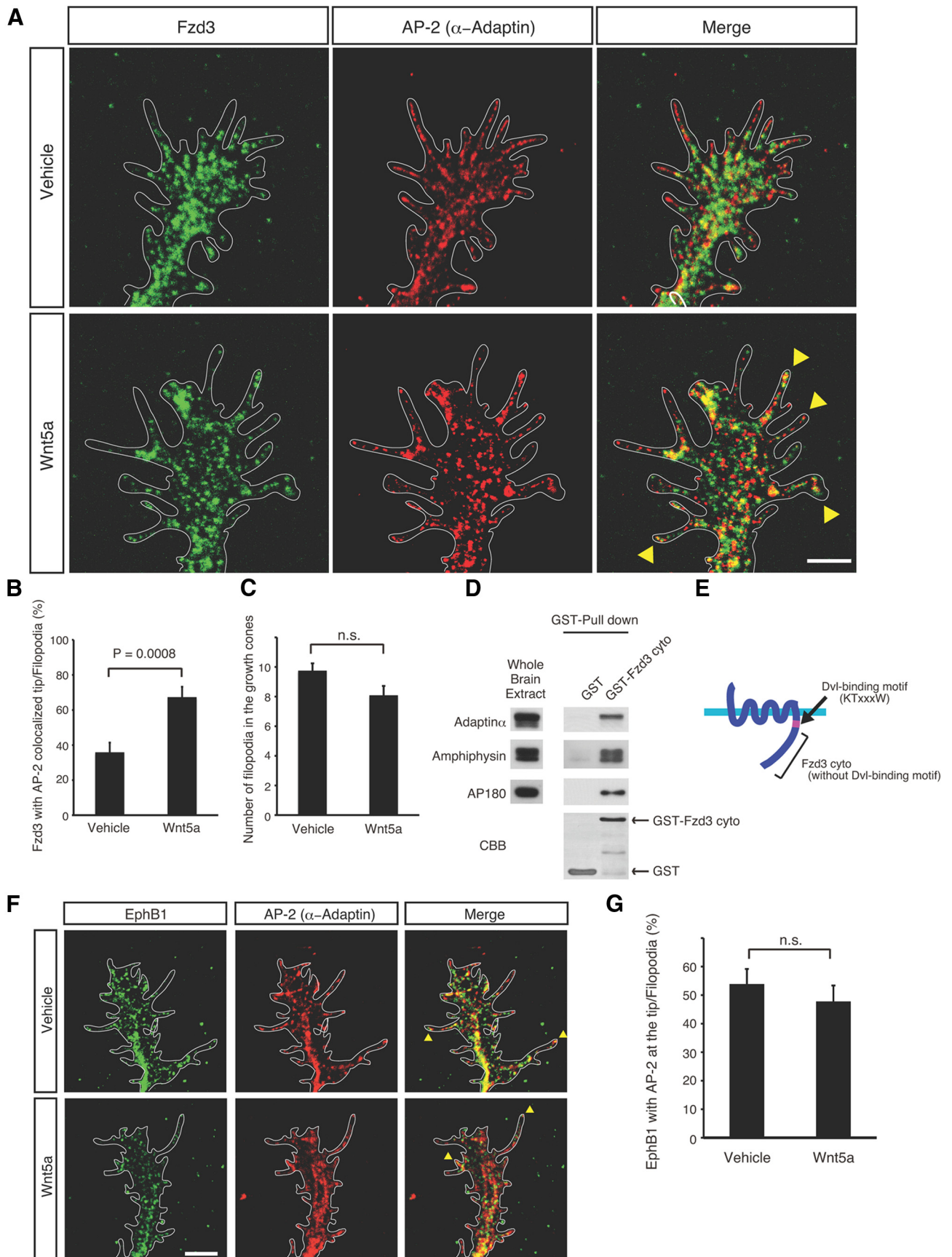


Figure 1. Frizzled3 is colocalized with AP-2 complexes at the tip of filopodia in the commissural axon growth cones. **A**, Immunostaining of endogenous Frizzled3 and α -Adaptin in the dissociated commissural axon growth cones. Endogenous Frizzled3 is colocalized with α -Adaptin at the tip of filopodia in Wnt5a-dependent manner. Scale bar, 5 μ m. **B**, Quantification of the colocalization of Frizzled3 and AP-2 complexes at the tips of filopodia in **A**. The percentage of filopodia with colocalized Frizzled and AP-2 puncta. Data are the mean \pm SEM. **C**, (Figure legend continues.)

sites (induced by Dishevelled1) mutated (Shafer et al., 2011). We routinely observed yellow mutant Frizzled3 (7A) vesicles, which moved back along the filopodia, suggesting that Frizzled3 endocytosis does not require hyperphosphorylation. On the other hand, once they have moved to the tips of filopodia, mutant Frizzled3 (7A) vesicles stayed at the tip of filopodia for a much longer time (Fig. 2D). This suggests that Frizzled3 phosphorylation is required for its efficient exocytosis. Consistent with this, FLAG signal intensity of Frizzled3 (7A) mutant is less than that of Frizzled3 WT, indicating that 7A mutation impairs Frizzled3 exocytosis (Fig. 2C; data are normalized by WT, $7A = 0.59 \pm 0.10$).

Wnt5a promotes endocytosis of Frizzled3 vesicles from filopodia tips

Using this new construct, we set out to test the behavior of Frizzled3 vesicles when PCP signaling is activated by Wnt5a, focusing on the tips of filopodia (Fig. 2F–I). We first characterized vesicle movement relative to the filopodia membrane, which may undergo elongation or shrinking. Some filopodia shrank very fast (within 2 frames/6 s), making it impossible to track vesicles inside. Therefore, we excluded those fast shrinking ones and only measured vesicle movement in slowly shrinking filopodia (at least 20–30 s). We also excluded overlapped filopodia, which are also often seen during imaging and would confuse the quantification. As shown in Figure 2, F and G, high-magnification columns, Frizzled3 vesicles move much faster than filopodia movement. Therefore, these vesicle movement reflect their trafficking within the filopodia, not the movement of the growing/shrinking of filopodia per se.

We then analyzed time-lapse imaging and found that Wnt5a addition (100 ng/ml) increased the number of Frizzled3 vesicles appearing from the tips and moving inward, away from the tips, in commissural axon growth cones, which correlates with elongation of filopodia, not the shrinking filopodia. In the absence of Wnt5a, the rate of outward movement/10 s was 0.33 ± 0.03 and inward movement/10 s was 0.89 ± 0.05 in growing filopodia, whereas in shrinking filopodia, outward movement/10 s was 0.78 ± 0.08 and inward movement/10 s was 0.46 ± 0.07 (Fig. 2H). In the presence of Wnt5a, outward movement/10 s was 0.29 ± 0.06 and inward movement/10 s was 1.07 ± 0.06 in growing filopodia, whereas in shrinking filopodia, outward movement/10 s was 0.81 ± 0.11 and inward movement/10 s was 0.44 ± 0.06 (Fig. 2H). Mutant Frizzled3 (7A), which cannot be hyperphosphorylated, on the other hand, does not respond to Wnt5a (Fig. 2I). These results suggest that Wnt5a promotes Frizzled3 endocytosis from filopodia tips of commissural growth cones.

Antagonistic interactions between Dishevelled2 and Dishevelled1 in Frizzled3 phosphorylation and trafficking

While testing the roles of all three Dishevelleds in regulating Frizzled3 phosphorylation, we uncovered an unexpected difference among the three Dishevelleds. In our previous study, we showed that Frizzled3 hyperphosphorylation, induced

by Dishevelled1, causes a mobility shift (Shafer et al., 2011). We found that, while Dishevelled3 also induces Frizzled3 hyperphosphorylation, Dishevelled2 does not (Fig. 3A). Consistent with this, we also found that Dishevelled1 and Dishevelled3 increase Frizzled3 cell-surface accumulation, but not Dishevelled2 (Fig. 3A). Furthermore, Dishevelled2 suppressed Dishevelled1-induced Frizzled3 hyperphosphorylation (Fig. 3B).

Frizzled3 hyperphosphorylation results in its cell-surface accumulation and inactivation of PCP signaling (Shafer et al., 2011). Therefore we hypothesized that Dishevelled2, but not Dishevelled1, mediates noncanonical Wnt signaling, such as PCP signaling. To address this, we developed the specific shRNA constructs against Dishevelled1 and Dishevelled2. We found that knockdown of Dishevelled2 suppressed Wnt5a-induced JNK activation (Fig. 3C). On the other hand, JNK was still activated in the Dishevelled1 knockdown cells (Fig. 3C). These results suggest that Dishevelled2 is necessary for Wnt-PCP signaling, whereas Dishevelled1 inhibits it.

aPKC inhibits Dishevelled1-induced Frizzled3 hyperphosphorylation

Our previous study showed that the localization and activity of Frizzled3 is regulated by its phosphorylation and aPKC is required for Wnt-mediated axon attraction and guidance (Wolf et al., 2008; Shafer et al., 2011). To investigate the interaction of aPKC and Frizzled3 trafficking, we tested the role of aPKC and found that constitutively active aPKC inhibits Dishevelled1-induced Frizzled3 hyperphosphorylation (Fig. 4A). PAR6 is a protein that forms a complex with aPKC in A-BP signaling. PAR6 and aPKC cooperatively inhibit Dishevelled1-induced Frizzled3 hyperphosphorylation (Fig. 4B).

We then investigated the interactions between aPKC and the Dishevelleds. The phosphorylation of T410 of PKC ζ causes the activation of this kinase. We found that Dishevelled2, not Dishevelled1, increased T410 phosphorylation in dissociated primary dorsal spinal cord neurons, suggesting that only Dishevelled2 activates aPKC (Fig. 4C). In these cultures, Wnt5a treatment increased T410 phosphorylation of aPKC as well as phosphorylated JNK (indicating JNK activation; Fig. 4D). These results suggest that Wnt5a-Dishevelled2 signaling indeed activates aPKC, which, in turn, inhibits Dishevelled1-induced Frizzled3 hyperphosphorylation.

Increased Frizzled3 hyperphosphorylation in *Celsr3* knock-out mice

To test whether Frizzled3 phosphorylation is important in PCP signaling *in vivo*, we investigated Frizzled3 phosphorylation state in *Celsr3* knock-out mice (Tissir et al., 2005). *Celsr3* is a homolog of *Drosophila flamingo* and encodes an essential component of PCP pathway in many contexts. We found, in whole-brain and spinal cord extracts from E11.5 *Celsr3* knock-out embryos, the upper band of Frizzled3 (hyperphosphorylated Frizzled3) was increased (Fig. 5A,B). Consistent with this, phosphorylation of JNK is diminished in both brain and spinal cord extracts from *Celsr3* knock-out mouse. This result indicates that Frizzled3 phosphorylation is an important regulatory mechanism for PCP signaling *in vivo*.

PCP signaling is required in commissural neurons for their proper anterior–posterior guidance

PCP components are expressed in commissural axon growth cones and *Frizzled3* and *Celsr3* knock-out mice, as well as a

(Figure legend continued.) Quantification of the number of filopodia in A. Data are the mean \pm SEM. D, Frizzled3 cytoplasmic region binds to a subset of endocytosis-related proteins. α -Adaptin, Amphiphysin, and AP180 are coprecipitated with GST-Fzd3cyto, but not GST control. E, The schematic diagram of GST-Fzd3cyto. GST-Fzd3cyto does not contain the Dishevelled binding motif (KTxxW). F, Immunostaining of endogenous EphB1 and α -Adaptin in the dissociated commissural axonal growth cones. G, Endogenous EphB1 is also colocalized with α -Adaptin at the tip of filopodia, although Wnt5a does not affect colocalization there. Scale bar, 5 μ m.

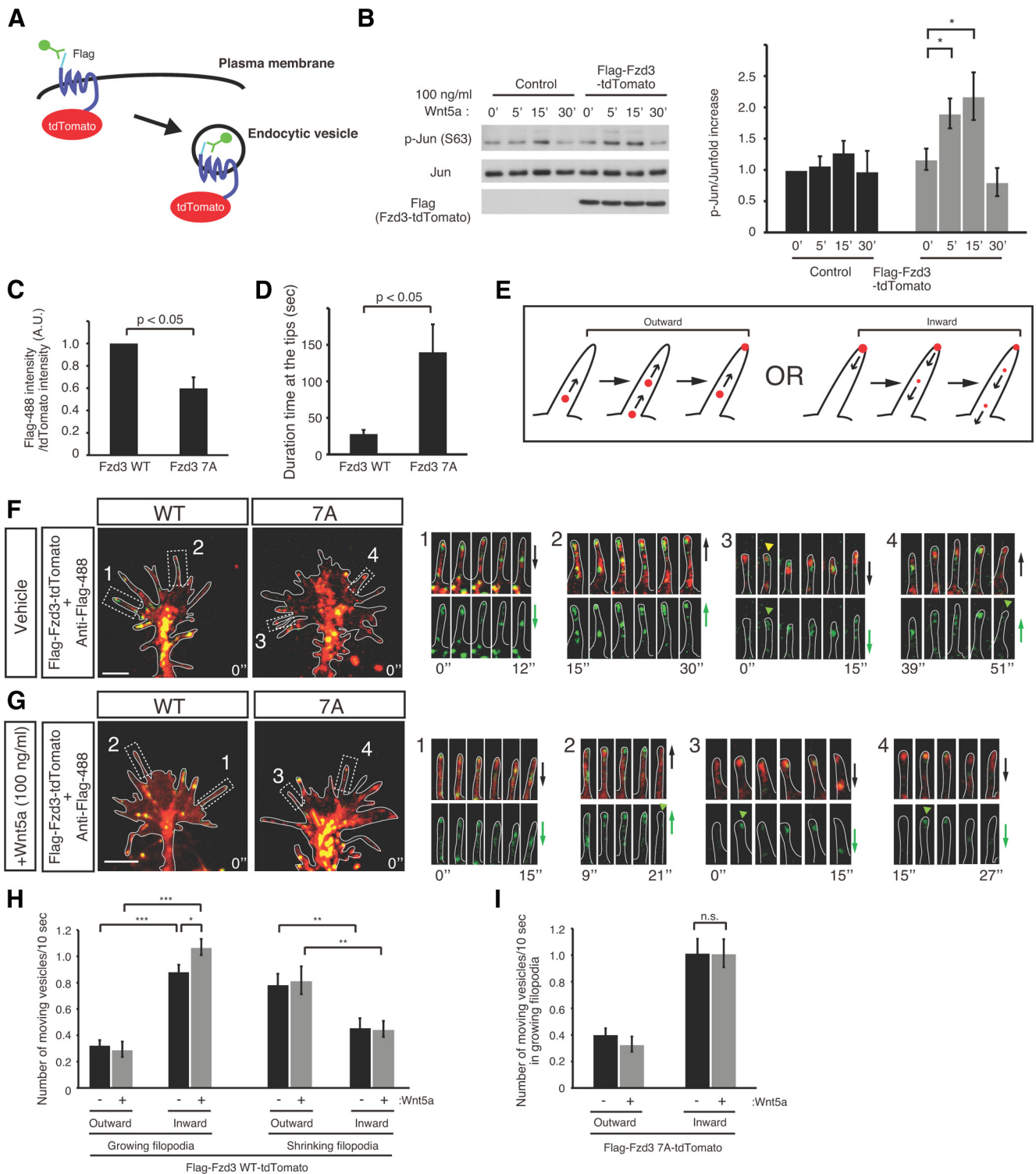


Figure 2. Frizzled3 undergoes endocytosis via the filopodia tips of commissural axon growth cones. **A**, Schematic diagram of a double labeling construct for Frizzled3. **B**, Flag-Frizzled3-tdTomato construct can mediate Wnt5a activation of JNK. Quantification data are the mean \pm SD of values. * p < 0.05. **C**, Quantification of FLAG signal intensity normalized by total Frizzled3 expression level (intensity of tdTomato; 15 min at 37°C). Data are the mean \pm SD. **D**, Quantification of the duration time of Frizzled3 WT and 7A mutant at the tip of filopodia. Frizzled3 7A mutant stays longer at the tips than WT. Data are mean \pm SD. **E**, Diagram for method of quantification of vesicle movement. **F**, Time-lapse imaging of FLAG-Frizzled3 WT and 7A mutant-tdTomato in the commissural axon growth cones in the absence of Wnt5a. Dash-line boxes indicate the position of high-magnification images. Yellow (green + red) vesicles represent “once” plasma membrane-localized, and currently internalized Frizzled3. Once internalized, some Frizzled3 WT is again transported back to the tips of filopodia, suggesting Frizzled3 WT is recycled. Row 1, inward movement; Row 2, outward movement; Row 3, Frizzled3 appeared at the tip and move inward; and Row 4, Frizzled3 move outward and disappeared at the tip. Scale bar, 5 μ m. **G**, Time-lapse imaging of FLAG-Frizzled3 WT and 7A mutant-tdTomato in the commissural axonal growth cones in the presence of Wnt5a (100 ng/ml). Row 1, inward movement; Row 2, Frizzled3 move outward and disappeared at the tip; and Rows 3 and 4, Frizzled3 appeared at the tip and move inward. Scale bar, 5 μ m. **H**, Quantification of the Frizzled3 WT-vesicle movement in the growing and shrinking filopodia. Wnt5a increases the inward movement (from tips to central domain) of Frizzled3 vesicles only in the growing filopodia. Data are the mean \pm SEM. * p < 0.05, ** p < 0.005, *** p < 10⁻⁵. **I**, Quantification of the Frizzled3 (7A)-vesicle movement in the growing filopodia. Wnt5a does not change Frizzled3 (7A) vesicle movement. Data are the mean \pm SEM.

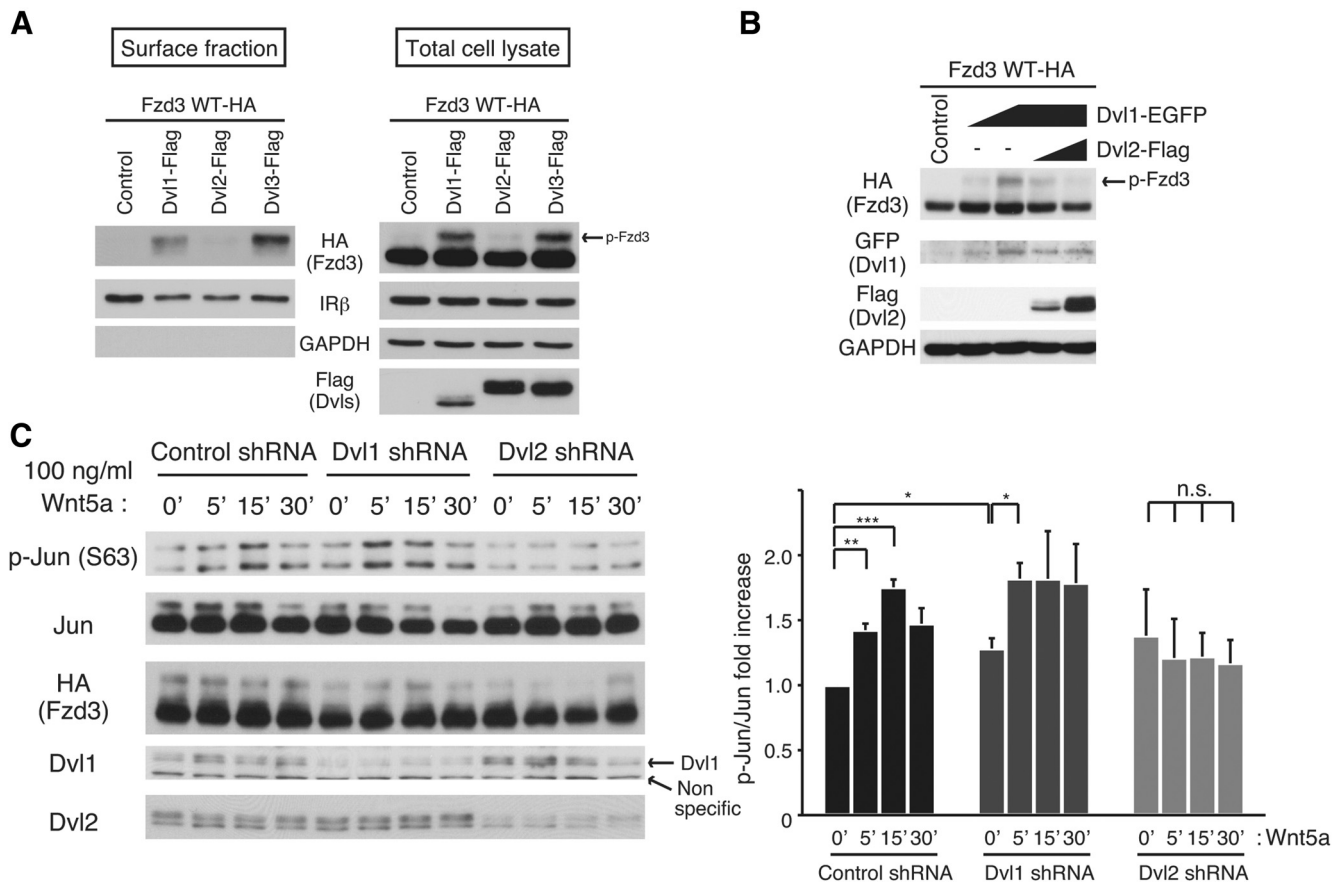


Figure 3. Dishevelled2 inhibits Dishevelled1-induced Frizzled3 hyperphosphorylation. **A**, Dishevelled1 and Dishevelled3 induce Frizzled3 cell-surface accumulation, but not Dishevelled2. GAPDH is used for cytoplasmic marker and IRβ (Insulin receptor β) is for cell-surface marker. **B**, Dishevelled2 inhibits Dishevelled1-induced Frizzled3 hyperphosphorylation (Dishevelled1: 0.1 μg or 0.3 μg; Dishevelled2: 0.1 μg or 0.3 μg). **C**, Dishevelled1 and Dishevelled2 have different roles in Wnt5a-induced JNK activation. Quantification data are the mean ± SD of values. **p* < 0.05, ***p* < 0.005, ****p* < 0.0005.

Vangl2 mutant mouse, *looptail*, display robust anterior–posterior guidance defects of spinal cord commissural axons (Lyuksyutova et al., 2003; Shafer et al., 2011; Fig. 5C). To directly test whether PCP signaling is required in commissural neurons but not the surrounding cells, such as the floor plate cells in the midline, we deleted *Celsr3* gene specifically in a subset of commissural axons using a *Celsr3* conditional allele crossed into *Wnt1-Cre* (Charron et al., 2003; Matsumoto et al., 2007; Zhou et al., 2008). *Wnt1-Cre* is expressed in the dorsal-most margin of the spinal cord, where commissural neuron cell bodies are located, and the recombination mediated by *Wnt1-Cre* starts at E9.5 (Charron et al., 2003).

First, we tested whether the *Celsr3* antibodies we generated recognize endogenous *Celsr3* specifically. In contrast to WT, *Celsr3* staining is almost lost in the dissociated *Celsr3* knock-out mouse commissural neurons (Fig. 5E), indicating that our *Celsr3* antibodies recognize *Celsr3* specifically. We then used these antibodies to verify the deletion of the *Celsr3* gene in commissural neurons in *Celsr3^{flox/flox};Wnt1-Cre* embryos. In E11.5 spinal cords of *Celsr3^{flox/flox}* embryos, we found that *Celsr3* is detected in the ventral and lateral funiculus, where postcrossing commissural axons grow (Fig. 5G, left). However, *Celsr3* staining in the ventral and lateral funiculus is lost in *Celsr3^{flox/flox};Wnt1-Cre* embryos (Fig. 5G, right).

We next examined the trajectory of commissural axons using L1 and TAG-1 staining (Fig. 5D, F). TAG-1 is expressed in the precrossing and crossing segments in the spinal cord, and L1 delineates postcrossing axons or growth cones. TAG-1

staining showed that the dorsoventral projection of precrossing commissural axons is normal in both *Celsr3^{flox/flox}* and *Celsr3^{flox/flox};Wnt1-Cre* spinal cords. After crossing, the axons grew within the ventral and lateral funiculus in both genotypes, as shown by L1 staining (Fig. 5F). We then analyzed anterior–posterior guidance using DiI tracing and found severe anterior–posterior guidance defects in *Celsr3^{flox/flox};Wnt1-Cre* embryos (Fig. 5H, I; *Celsr3^{flox/+}* = 85.7 ± 13.9%, *Celsr3^{flox/flox}* = 85.2 ± 13.5%, *Celsr3^{flox/+};Wnt1-Cre* = 81.1 ± 16.4%, and *Celsr3^{flox/flox};Wnt1-Cre* = 16.9 ± 4.5%). These results demonstrate that *Celsr3* in the commissural neurons is important for the commissural axon anterior turning.

Arf6 is the small GTPase, which regulates Frizzled3 recycling

To further investigate how Frizzled3 trafficking is regulated and whether Frizzled3 recycling is necessary for axon guidance, we tested a number of Rabs and Arf6, which regulate the trafficking of many different kinds of receptor tyrosine kinases, G-protein-coupled receptors, and other types of cell-surface proteins (cadherins, integrins, etc.; Jackson and Casanova, 2000; Santy and Casanova, 2001). First, we performed coimmunoprecipitation experiments to investigate whether Rabs or Arf6 can interact with Frizzled3. We found that Frizzled3 coimmunoprecipitated with Arf6-EGFP, but not with EGFP-Rab4, 5, 8, or 11 (Fig. 6A). Furthermore, Frizzled3 coimmunoprecipitated with Arf6 WT and T157A mutant, a fast cycling form and more active mutant than WT (Santy, 2002), more efficiently

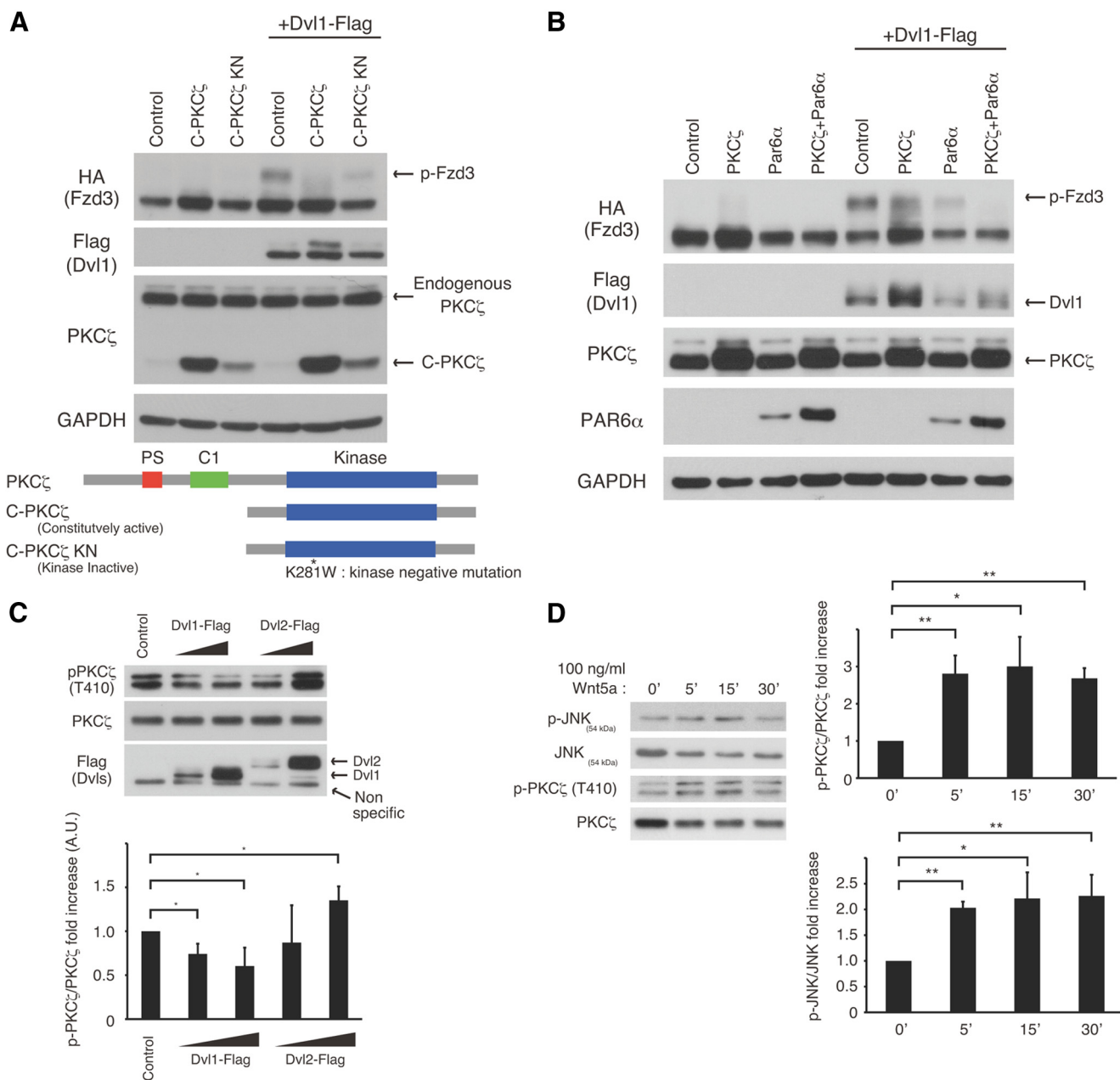


Figure 4. aPKC/PAR6, activated by Disvelled2, inhibits hyperphosphorylation of Frizzled3 induced by Disvelled1. **A**, Constitutively active aPKC inhibits Disvelled1-induced Frizzled3 phosphorylation. **B**, PAR6 and aPKC cooperatively inhibit Disvelled1-induced Frizzled3 phosphorylation. **C**, Disvelled2, not Disvelled1, activates aPKC (Disvelled1: 0.1 μ g or 0.3 μ g; Disvelled2: 0.1 μ g or 0.3 μ g). Quantification data are the mean \pm SD of values. * p < 0.05. **D**, Wnt5a activates aPKC and JNK in commissural neurons. Quantification data are the mean \pm SD of values from three independent experiments; * p < 0.05, ** p < 0.005.

than with Arf6 T27N mutant, which can bind with only GDP and acts as a dominant-negative (Fig. 6B). We next investigated whether Frizzled3 phosphorylation affects the interaction between Arf6 and Frizzled3. We found that Arf6 was coimmunoprecipitated with 7A mutant, seven phosphorylation sites of which (induced by Disvelled1) are mutated, more efficiently than with WT (Fig. 6C). This result suggests that Frizzled3 phosphorylation may inhibit the interaction between Arf6 and Frizzled3 and thus inhibits its endocytosis.

To test whether Arf6 is involved in Frizzled3 trafficking, we analyzed the cell-surface level of Frizzled3 by using the cell-surface biotinylation and avidin pull-down system. We found that Arf6 T157A constitutively-active mutant suppressed Disvelled1-

induced Frizzled3 surface accumulation and hyperphosphorylation (Fig. 6D). Consistent with this, dominant-negative Arf6 (DN-Arf6; T27N mutant) expression significantly enhanced Frizzled3 cell-surface accumulation even without Disvelled1 overexpression (Fig. 6E). These results suggest that Arf6 regulates Frizzled3 recycling. We also noticed a lower band in the left (control) lane. Therefore, we performed phosphatase assay using surface fraction. The upper band in surface fraction was completely removed by phosphatase treatment (Fig. 6F). Interestingly, this lower Frizzled3 band, which is higher than the lowest band in the total extract, is still there, suggesting that the lower band in the surface fraction represents other modification (Fig. 6F). Because it has been reported that Frizzled7 and 8 are glycosylated (Yamamoto et

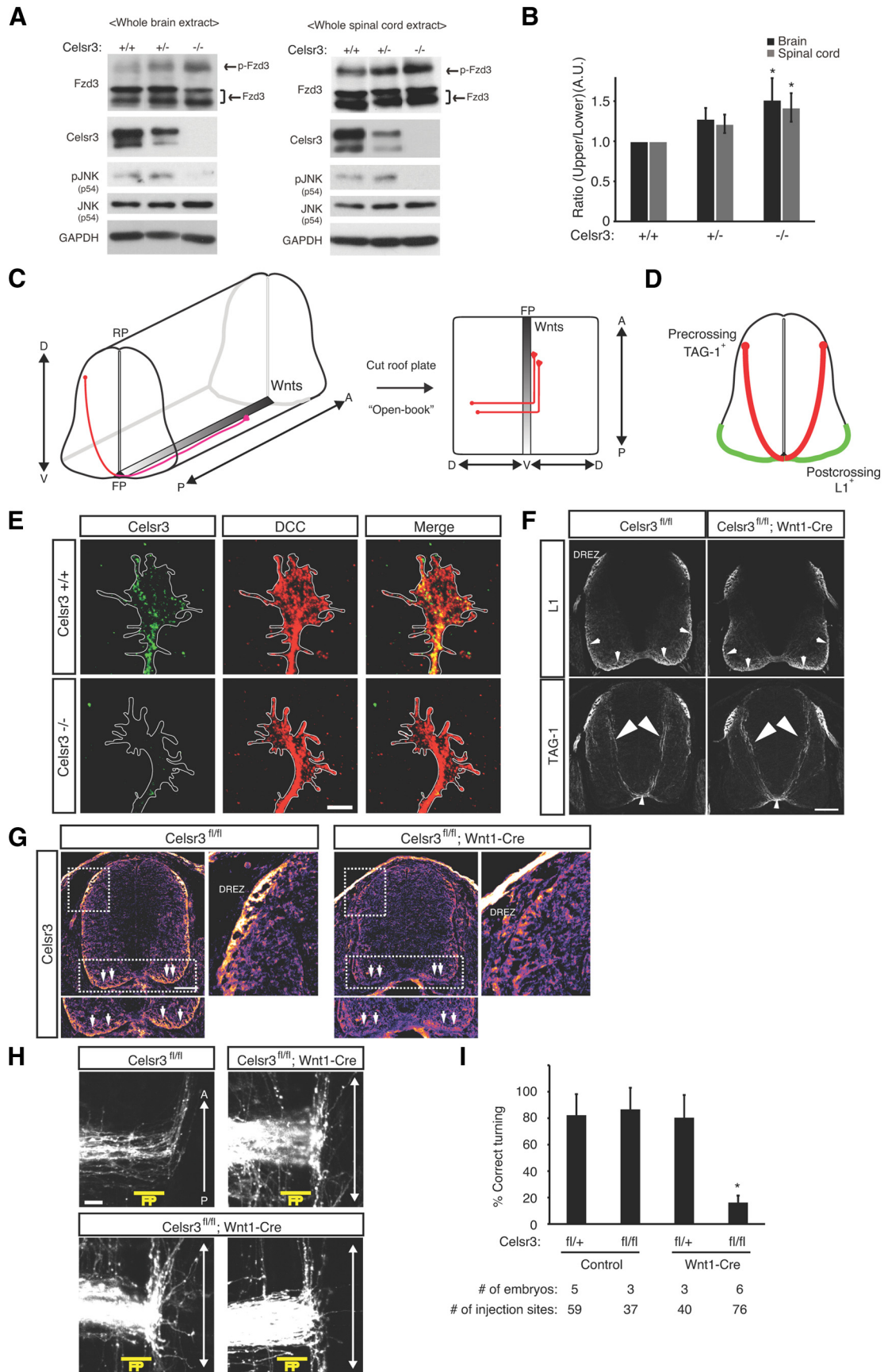


Figure 5. Increased Frizzled3 hyperphosphorylation in *Celsr3* knock-out mice and requirement of *Celsr3* in commissural neurons. **A**, Increase of Frizzled3 hyperphosphorylation in *Celsr3* knock-out mouse (E11.5). **B**, Quantification of the ratio between phosphorylated Frizzled3 and nonphosphorylated Frizzled3 in *Celsr3* knock-out mice brain and spinal cord tissue lysate. Intensities of upper bands are divided by that of lower bands and normalized by WT (+/+). The number of +/+ embryos = 9, +/- = 6, -/- = 5 from three different litters. (Figure legend continues.)

al., 2005), this Frizzled3 mobility shift might also be due to glycosylation. Therefore we tested this possibility and found that PNGase F, an amidase that cleaves *N*-linked glycans from glycoproteins, further fastened both higher and lower Frizzled3 bands, suggesting that all Frizzled3 on the plasma membrane are glycosylated and some of them are phosphorylated. Importantly, constitutively active and WT Arf6 greatly also increases Frizzled3 mobility on the gel (Fig. 6D). They increased the lowest band, which appears to correspond to the unmodified Frizzled3, suggesting that Arf6 might regulate not only phosphorylation but also glycosylation.

Because Frizzled3 endocytosis is required for Wnt-induced PCP signal activation (Yu et al., 2007; Sato et al., 2010), we tested whether Arf6 is involved in Wnt-PCP signaling. In control cells, Wnt5a treatment increased phosphorylation of c-Jun. However, in DN-Arf6-expressing cells, Wnt5a treatment did not increase, but rather decreased the phosphorylation of c-Jun very rapidly, suggesting that Arf6 activity is required for Wnt5a-induced PCP signal activation (Fig. 6G). These data suggest that Arf6 mediates Frizzled3 endocytosis and PCP signaling.

Arf6 is required for Wnt-mediated commissural axon outgrowth

We previously showed that Wnt5a promotes commissural axon elongation via PCP signaling (Shafer et al., 2011). Therefore, we tested whether Arf6 is involved in Wnt5a-induced commissural axon elongation. In control shRNA-expressing neurons, Wnt5a treatment significantly promoted commissural axon outgrowth. On the other hand, Arf6 knockdown abolished Wnt5a-induced commissural axon outgrowth (Fig. 7A,B; data are normalized by Control shRNA, Control shRNA + Wnt5a = 1.43 ± 0.03 , Arf6 shRNA = 1.33 ± 0.06 , and Arf6 shRNA + Wnt5a = 1.06 ± 0.11). We validated the knockdown efficiency of shRNA targeting rat Arf6 by using expression plasmid encoding rat Arf6-EGFP (Fig. 7C).

After analyzing Arf6 trafficking in the growth cones, we found that, like Frizzled3, Arf6-EGFP vesicles are also present at the tips of growth cone filopodia (Fig. 7D, left and box1). Moreover, the small Arf6-EGFP-positive vesicles also appear from the tips and move inward along filopodia (Fig. 7D). Importantly, inward

movement of Arf6-EGFP vesicles is observed much more frequently in growing filopodia, but not as frequently in shrinking filopodia (Fig. 7D, right graph). This result suggests that Frizzled3 recycling mediated by Arf6 does initiate more frequently in extending/growing filopodia than in shrinking ones.

Based on our results, we hypothesize that Dishevelled1 inhibits Wnt/PCP signaling by keeping Frizzled3 in a hyperphosphorylated state and on plasma membrane (Fig. 7, left). PCP signaling can be activated by Wnts and the activated Dishevelled2 can remove inhibition of PCP signaling by activating aPKC, which inhibits Dishevelled1, thus causing signal amplification. And Arf6 is required for Frizzled3 endocytosis once PCP signaling is activated (Fig. 7E, right).

Frizzled3 is endocytosed asymmetrically in Wnt5a gradient

To test whether the tightly regulated Frizzled3 endocytosis mediates growth cone turning, we exposed commissural axon growth cones to a Wnt5a gradient using the Dunn chamber (Yam et al., 2009). Commissural neurons were grown in culture and then exposed to a gradient of Wnt5a. We tested our system and found that it takes ~20 min to form the gradient from end to end using 40 kDa tetramethylrhodamine dextran (data not shown). Thirty minutes after the addition of Wnt5a or BSA (as a control), commissural neurons were fixed. Thus, these growth cones would have been in a stable gradient for ~10 min. We then immunostained these growth cones with Frizzled3 and α -Adaptin, a subunit of AP-2 complex. In control BSA gradient, Frizzled3 and AP-2 colocalized tips were equally distributed in both proximal and distal side (Fig. 8A–C), suggesting that Frizzled3 is endocytosed randomly at the filopodia tips in the absence of Wnts gradient. In contrast, there was a significant bias for a proximal (closer to Wnt5a source) distribution of Frizzled3 and AP-2 colocalized tips. (Fig. 8A–C). In this time frame of our experiments, Wnt5a gradient did not affect filopodia formation in both proximal and distal side (Fig. 8D). This result suggests that Frizzled3 is endocytosed more frequently in the side of the growth cones exposed to higher Wnt5a level.

To further investigate whether the distribution of activated aPKC, a downstream target of Wnt5a and Dishevelled2, also shows asymmetry in the Wnt5a gradient, we stained for activated aPKC marker (phospho-PKC ζ (T410)). We found that active aPKC (phospho-PKC ζ (T410)) was enriched in the proximal side exposed to higher Wnt5a level than the distal side in the growth cones (Fig. 8E,F). Together, these results suggest that Wnt5a gradient causes asymmetric endocytosis of Frizzled3 and aPKC activation in the growth cones, which may be essential for growth cone turning toward higher Wnt5a concentration (Fig. 8G).

Discussion

An emerging theme in growth cone guidance is that PCP signaling pathway may be a widely used mechanism for mediating directional control of axon growth (Zou, 2012). How PCP signaling components direct growth cone turning is still poorly known. We show here that Frizzled3 endocytosis through the tips of growth cone filopodia, tightly regulated by its phosphorylation state, is essential for Wnt-mediated growth cone turning (Fig. 8G). Our earlier studies showed that aPKC, a key component of apical-basal polarity (A-BP) signaling, also mediates Wnt attractions and anterior–posterior guidance of commissural axons (Wolf et al., 2008). We found here that aPKC inhibits Dishevelled1-induced Frizzled3 hyperphosphorylation and thus

←

(Figure legend continued.) * $p < 0.05$. **C**, A schematics of commissural axon pathfinding in mouse E11.5 or rat E13 spinal cords. Spinal cords are dissected and splayed open from the roof plate to give rise to open-book preparation allowing the visualization of commissural axons pathfinding before, during and after midline crossing of the spinal cords are prepared. **D**, Schematics of an mouse E11.5 or rat E13 spinal cord transverse section. Spinal cord is bilaterally symmetrical at this stage and there are commissural neurons and their axons on both sides of the midline. Green is the TAG-1-positive precrossing segment approaching the ventral midline, and red indicates the L1-positive postcrossing axon segment after midline crossing. **E**, Anti-Celsr3 antibodies recognize Celsr3 specifically. Scale bar, 5 μ m. **F**, TAG1 immunostaining shows normal dorsoventral trajectory in both genotypes, and L1 immunostaining shows commissural axons can grow within the ventral and lateral funiculus in both genotypes. Scale bar, 100 μ m. **G**, Celsr3 is expressed in postcrossing commissural axons. Transverse sections of E11.5 spinal cords of Celsr3^{flox/flox};Wnt1-Cre and Celsr3^{flox/flox} (as WT) littermate embryos were stained with anti-Celsr3 antibodies. The images are pseudocolored heat map of Celsr3 immunostainings. Dash-line boxes indicate the position of high-magnification images. Arrows indicate postcrossing segments. Scale bar, 100 μ m. **H**, Anterior–posterior guidance defects in Celsr3^{flox/flox};Wnt1-Cre embryos. Commissural axons were labeled by lipophilic Dil injection into the “open-booked” dorsal spinal cord explants of Celsr3^{flox/flox};Wnt1-Cre and Celsr3^{flox/flox} (as WT) littermate embryos. Scale bars: 50 μ m. **I**, Quantification of open-book assay experiments in **C**. The graph represents the frequency of the anterior turning (correct turning) as a percentage of all injection sites. * $p = 0.00001$ compared with other three genotypes. D, dorsal; V, ventral; A, anterior; P, posterior; RP, roof plate; FP, floor plate; DREZ, dorsal root entry zone.

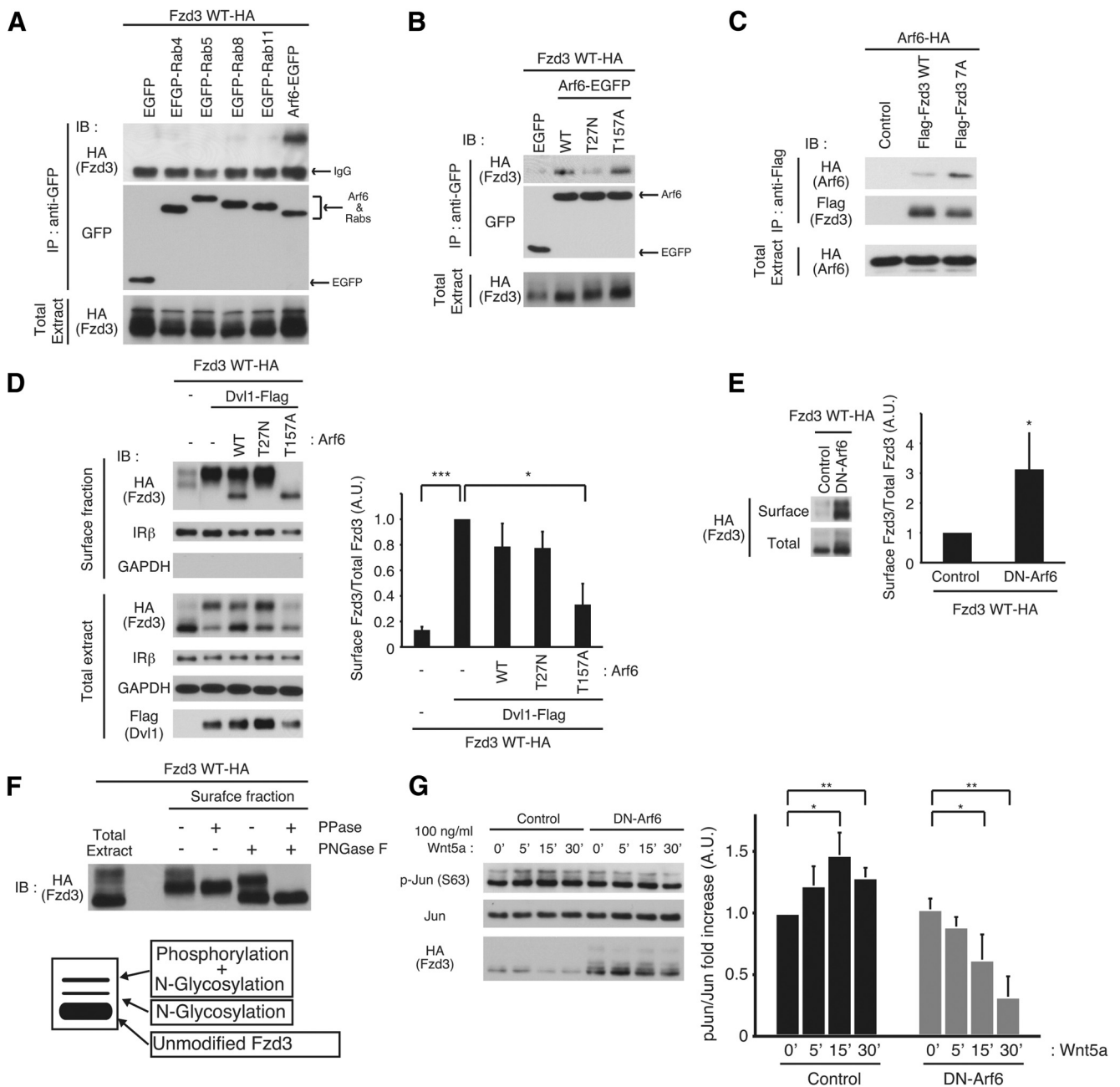


Figure 6. Arf6 mediates Frizzled3 endocytosis and Wnt-PCP signaling. **A**, Arf6 interacts with Frizzled3. **B**, Frizzled3 interacts with Arf6 WT and T157A mutant, and less with T27N mutant. **C**, Arf6 preferentially interacts with Frizzled3 (7A) mutant. **D**, Arf6 T157A mutant suppresses Dishevelled1-induced Frizzled3 hyperphosphorylation and cell-surface accumulation. GAPDH is used for cytoplasmic marker and IRβ (Insulin receptor β) is for cell-surface marker. **E**, DN-Arf6 induces Frizzled3 cell-surface accumulation. **F**, Modification of Frizzled3 on cell surface. **G**, Arf6 activity is required for Wnt5a-induced PCP signal activation. Quantification data in **D**, **E**, and **G**, are the mean ± SD of values from three independent experiments. **p* < 0.05, ***p* < 0.01, ****p* < 0.001.

promotes Frizzled3 endocytosis. Activated aPKC is also localized asymmetrically in growth cones in a Wnt gradient (Fig. 8G). A-BP and PCP are two fundamental cellular properties, essential to the morphology and function of many classes of cells (Karner et al., 2006; Wang and Nathans, 2007; Zallen, 2007; Knoblich, 2008). These cell polarity qualities are particularly prominent in epithelial tissues, along perpendicular axes, but are also widely present in tissues from other germ layers (Karner et al., 2006; Zallen, 2007; Goodrich and Strutt, 2011). The findings that these two cell polarity signaling pathways are essential for axon guidance opens a new avenue to study growth signaling mechanisms leading to steering (Zou, 2012).

The growth cone is divided into distinct compartments of individual filopodia (peripheral domain) and the central domain. We show that Dishevelled1 blocks Wnt/PCP signaling by keeping Frizzled3 in hyperphosphorylated state and on plasma membrane (Fig. 7E). Dishevelled2, which activates aPKC, inhibits Dishevelled1. Therefore, once PCP signaling is activated in a subset of filopodia, as marked by high levels of Vangl2, PCP signal can be amplified by this antagonistic interaction between Dishevelled2 and Dishevelled1 (Fig. 7F). This positive feedback mechanism amplifies Wnt-PCP signaling and may help sensitize the growth cone in shallow gradients of Wnts along the anterior–posterior axis.

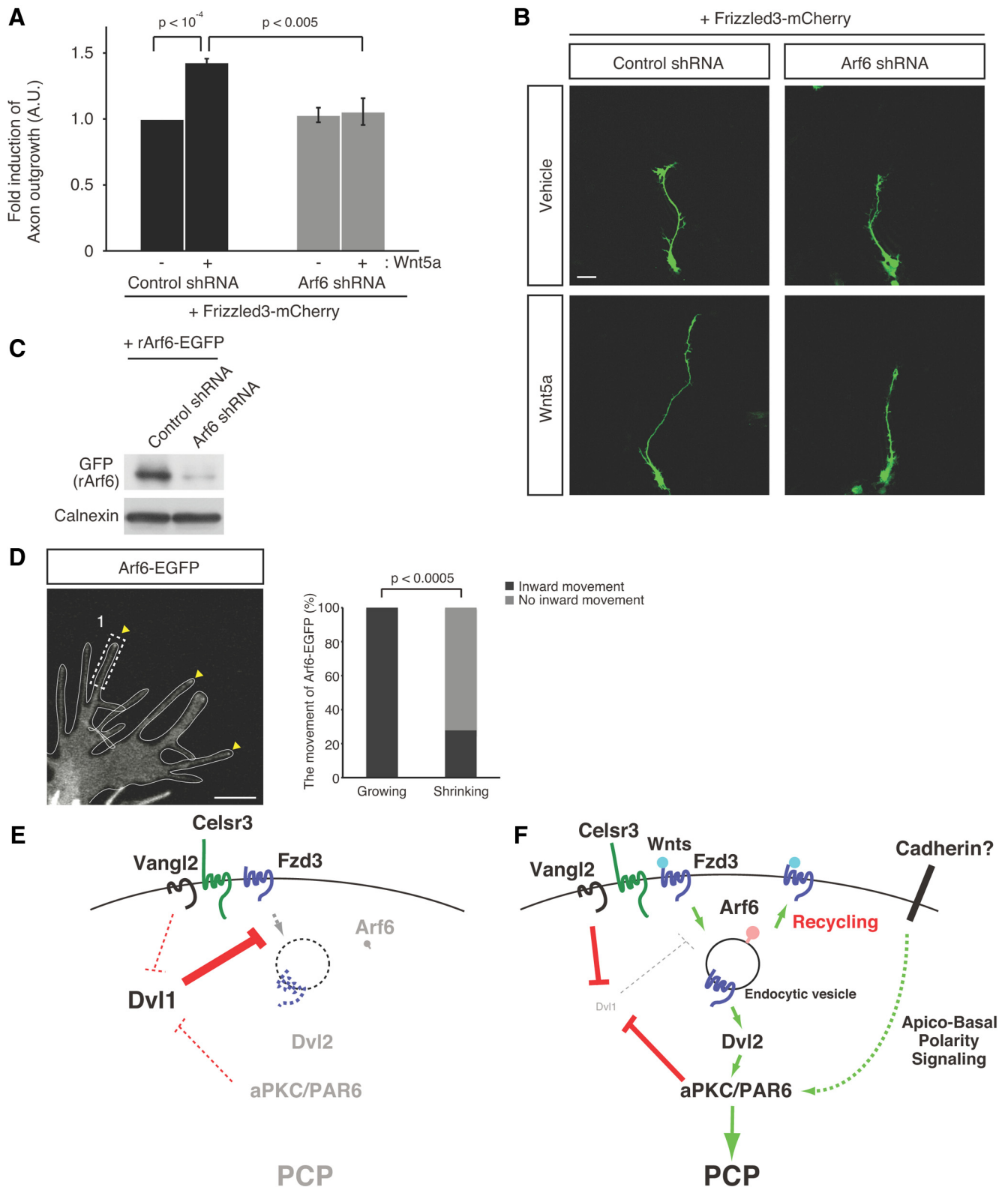


Figure 7. Arf6 mediates Wnt5a-induced commissural axon outgrowth. **A**, Arf6 is required for Wnt5a-induced commissural axon outgrowth. Quantification data are the mean \pm SD of values from three independent experiments. **B**, Images of commissural neurons expressing control shRNA or Arf6 shRNA in the absence or presence of Wnt5a. Scale bar, 10 μ m. **C**, The efficiency of Arf6 knockdown. **D**, Arf6-EGFP trafficking in the commissural growth cones. Arf6-EGFP accumulates at the tips of filopodia in the commissural axonal growth cones. The inward movement of Arf6-EGFP vesicles is observed more frequently in the growing filopodia than in the shrinking filopodia. **E, F**, A model for signal amplification. In the absence of Wnt, Dishevelled1 inhibits Frizzled3 endocytosis by inducing Frizzled3 hyperphosphorylation. Upon Wnt binding, Frizzled3 is endocytosed and activates the Dishevelled2-aPKC/PAR6 axis. aPKC then inhibits Dishevelled1. In the meantime, Vangl2 also inhibits Dishevelled1. As a result, more Frizzled3 is endocytosed and activates downstream signaling, which then in turn further removes inhibition by Dishevelled1. Arf6 mediates Frizzled3 endocytosis and its essential roles in PCP signaling activation. Meanwhile, A-BP polarity signaling pathway is also involved in aPKC regulation, suggesting A-BP signaling also regulates PCP signaling.

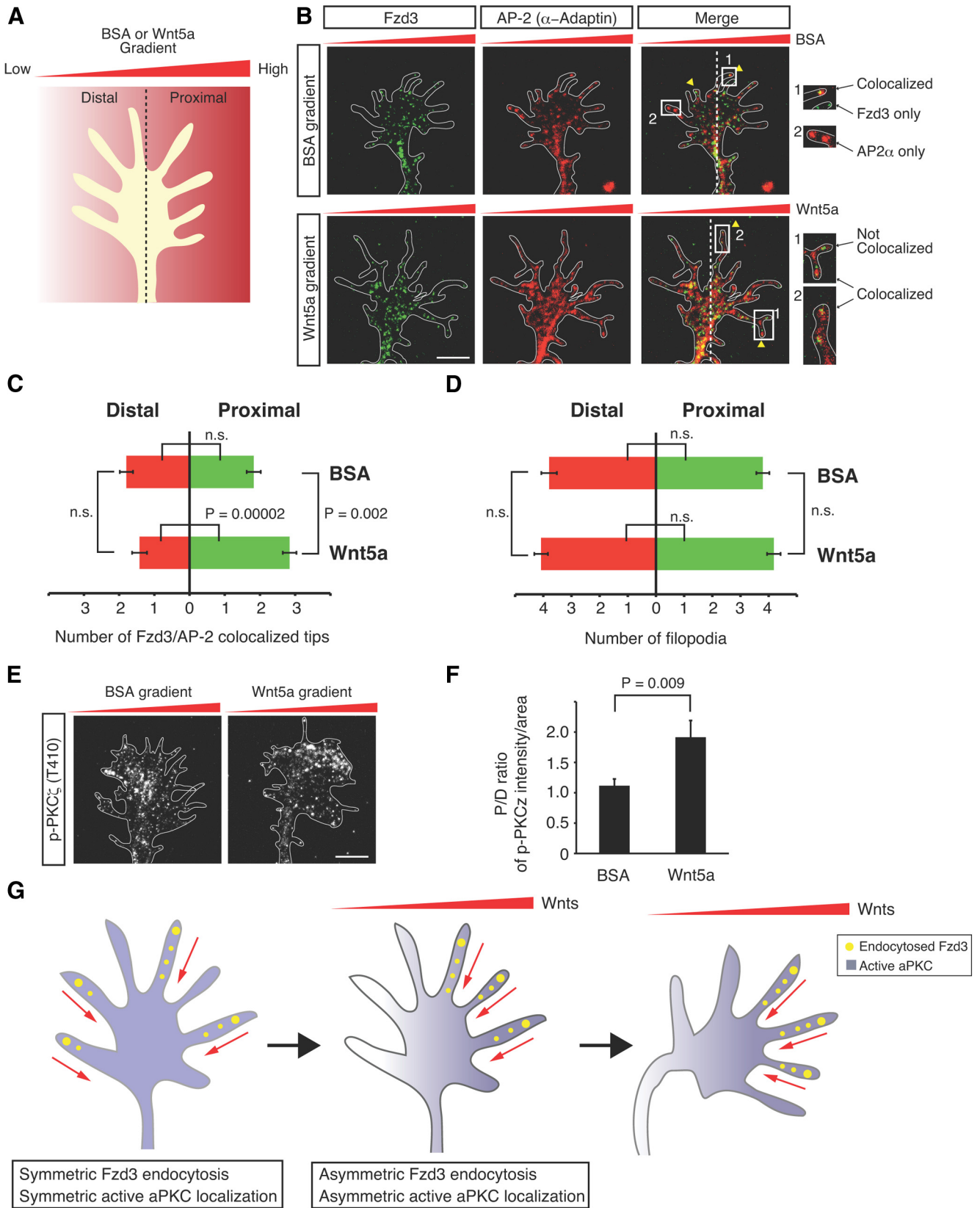


Figure 8. Frizzled3 endocytosis in a Wnt5a gradient. **A**, Schematics of experimental design to expose commissural axon growth cones to Wnt5a gradient using the Dunn chamber. Growth cones perpendicular to the gradient were selected and divided into a “proximal” and “distal” side. **B**, Immunostaining of endogenous Frizzled3 and α -Adaptin in the dissociated commissural axonal growth cones exposed to BSA or Wnt5a gradient in the Dunn chamber. Endogenous Frizzled3 is colocalized with α -Adaptin at the tip of filopodia more frequently in the proximal side. Scale bar, 5 μ m. **C**, Quantification data about the colocalization of Frizzled3 and AP-2 at the tips of filopodia in **B**. Data are the mean \pm SEM. **D**, Quantification data about the number of filopodia in **B**. Data are the mean \pm SEM. **E**, Immunostaining of phospho-PKC ζ (T410) in the dissociated commissural axonal growth cones exposed to BSA or Wnt5a gradient in the Dunn chamber. Phospho-PKC ζ is more abundant in the proximal side. Scale bar, 5 μ m. **F**, Quantification data about P/D ratio of phospho-PKC ζ (T410) intensity/area in **B**. Data are the (Figure legend continues.)

In searching for small GTPases, which may regulate Frizzled3 trafficking, we found that Arf6 regulates Frizzled3 endocytosis and preferably binds to nonphosphorylated Frizzled3. Arf6 is required for Wnt5a-mediated PCP signaling and commissural axon outgrowth promoted by Wnt/PCP signaling. Arf6 is known to mediate rapid endocytosis. This is also consistent with our observation that Frizzled3 is very rapidly endocytosed via the tips of growth cones. This may be necessary for growth cones to bring in information from the environment for making decisions for the direction of turning (Fig. 8G). Remarkably, using Arf6-EGFP as an indicator for endocytic vesicles, we found that the inward movement of Arf6 vesicles correlates with filopodia extension. This provides additional support to the hypothesis that Frizzled3 endocytosis and inward movement bring in PCP signal to likely regulate actin and microtubule dynamics.

In commissural axon turning, growth cones are organized in a plane parallel to the floor plate and turn anteriorly as a group after crossing the floor plate. The growth cones of commissural neurons which are born at the same time are within close proximity. It takes hours (8–9) to cross the midline and an additional 1–2 h to turn anteriorly (Zou lab, unpublished results). Filopodia of commissural axon growth cones have plenty of time to interact with each other. Therefore, this global anterior turning of a “sheet” of commissural axons is highly reminiscent of planar polarity in epithelia (Zou, 2012). If such growth cone–growth cone interaction exists and is important for proper turning, Cesl3 would be a strong candidate for mediating this interaction. If this actually occurs, a sheet of axons can sample a longer distance along the anterior–posterior axis, thus a greater concentration drop than individual growth cones. This is an interesting plausible mechanism of how shallow gradient of guidance cues are efficiently deflected.

In addition to the spinal cord commissural axons, serotonergic and dopaminergic axons, originating from the hindbrain and midbrain, respectively, also orient their axons along the anterior–posterior axis under the control of Wnt/planar cell polarity signaling (Fenstermaker et al., 2010; Blakely et al., 2011). Studies in *Drosophila* also revealed consistent mechanisms that PCP signaling is essential for proper growth and guidance of mushroom body neuron and dorsal cluster neuron axons (Mrkusich et al., 2011; Shimizu et al., 2011). Additional studies in invertebrates showed that PCP signaling can regulate neurite formation in *Caenorhabditis elegans* and axon branch extension in *Drosophila* (Sanchez-Alvarez et al., 2011; Ng, 2012). A Wnt receptor, Ryk/Derailed, first found to be a converted repulsive receptor in *Drosophila* and rodents, has been shown recently as a regulator of PCP signaling (Yoshikawa et al., 2003; Liu et al., 2005; Keeble et al., 2006; Schmitt et al., 2006; Liu et al., 2008; Li et al., 2009; Andre et al., 2012; Macheda et al., 2012). These studies suggest that PCP signaling may be a commonly used pathway for directional control of axon growth and thus making Wnt/PCP signaling an excellent system to study growth cone steering mechanisms (Zou, 2012).

←

(Figure legend continued.) mean \pm SEM. **G**, A working hypothesis of commissural axonal growth cone turning according to Wnt gradients. In the absence of Wnts gradient, Frizzled3 is endocytosed randomly through the filopodia tips and active aPKC is distributed uniformly (left growth cone). In a Wnt gradient, Frizzled3 endocytosis occurs more frequently in the proximal side and causes more aPKC activation (middle growth cone).

References

- Andre P, Wang Q, Wang N, Gao B, Schilit A, Halford MM, Stacker SA, Zhang X, Yang Y (2012) The Wnt coreceptor Ryk regulates Wnt/planar cell polarity by modulating the degradation of the core planar cell polarity component Vangl2. *J Biol Chem* 287:44518–44525. [Medline](#)
- Bashaw GJ, Klein R (2010) Signaling from axon guidance receptors. *Cold Spring Harb Perspect Biol* 2:a001941. [CrossRef Medline](#)
- Blakely BD, Bye CR, Fernando CV, Horne MK, Macheda ML, Stacker SA, Arenas E, Parish CL (2011) Wnt5a regulates midbrain dopaminergic axon growth and guidance. *PLoS One* 6:e18373. [CrossRef Medline](#)
- Charron F, Stein E, Jeong J, McMahon AP, Tessier-Lavigne M (2003) The morphogen sonic hedgehog is an axonal chemoattractant that collaborates with netrin-1 in midline axon guidance. *Cell* 113:11–23. [CrossRef Medline](#)
- Fenstermaker AG, Prasad AA, Bechara A, Adolfs Y, Tissir F, Goffinet A, Zou Y, Pasterkamp RJ (2010) Wnt/Planar cell polarity signaling controls the anterior-posterior organization of monoaminergic axons in the brainstem. *J Neurosci* 30:16053–16064. [CrossRef Medline](#)
- Goodrich LV, Strutt D (2011) Principles of planar polarity in animal development. *Development* 138:1877–1892. [CrossRef Medline](#)
- Jackson CL, Casanova JE (2000) Turning on ARF: the Sec7 family of guanine-nucleotide-exchange factors. *Trends Cell Biol* 10:60–67. [CrossRef Medline](#)
- Karner C, Wharton KA, Carroll TJ (2006) Apical-basal polarity, Wnt signaling and vertebrate organogenesis. *Semin Cell Dev Biol* 17:214–222. [CrossRef Medline](#)
- Keeble TR, Halford MM, Seaman C, Kee N, Macheda M, Anderson RB, Stacker SA, Cooper HM (2006) The Wnt receptor Ryk is required for Wnt5a-mediated axon guidance on the contralateral side of the corpus callosum. *J Neurosci* 26:5840–5848. [CrossRef Medline](#)
- Knoblich JA (2008) Mechanisms of asymmetric stem cell division. *Cell* 132:583–597. [CrossRef Medline](#)
- Li L, Hutchins BI, Kalil K (2009) Wnt5a induces simultaneous cortical axon outgrowth and repulsive axon guidance through distinct signaling mechanisms. *J Neurosci* 29:5873–5883. [CrossRef Medline](#)
- Liu Y, Shi J, Lu CC, Wang ZB, Lyuksyutova AI, Song XJ, Zou Y (2005) Ryk-mediated Wnt repulsion regulates posterior-directed growth of corticospinal tract. *Nat Neurosci* 8:1151–1159. [CrossRef Medline](#)
- Liu Y, Wang X, Lu CC, Kerman R, Steward O, Xu XM, Zou Y (2008) Repulsive Wnt signaling inhibits axon regeneration after CNS injury. *J Neurosci* 28:8376–8382. [CrossRef Medline](#)
- Lyuksyutova AI, Lu CC, Milanesio N, King LA, Guo N, Wang Y, Nathans J, Tessier-Lavigne M, Zou Y (2003) Anterior-posterior guidance of commissural axons by Wnt-frizzled signaling. *Science* 302:1984–1988. [CrossRef Medline](#)
- Macheda ML, Sun WW, Kugathasan K, Hogan BM, Bower NI, Halford MM, Zhang YF, Jacques BE, Lieschke GJ, Dabdoub A, Stacker SA (2012) The Wnt receptor Ryk plays a role in mammalian planar cell polarity signaling. *J Biol Chem* 287:29312–29323. [CrossRef Medline](#)
- Matsumoto Y, Irie F, Inatani M, Tessier-Lavigne M, Yamaguchi Y (2007) Netrin-1/DCC signaling in commissural axon guidance requires cell-autonomous expression of heparan sulfate. *J Neurosci* 27:4342–4350. [CrossRef Medline](#)
- Mrkusich EM, Flanagan DJ, Whittington PM (2011) The core planar cell polarity gene prickle interacts with flamingo to promote sensory axon advance in the *Drosophila* embryo. *Dev Biol* 358:224–230. [CrossRef Medline](#)
- Ng J (2012) Wnt/PCP proteins regulate stereotyped axon branch extension in *Drosophila*. *Development* 139:165–177. [CrossRef Medline](#)
- Sanchez-Alvarez L, Visanuvimol J, McEwan A, Su A, Imai JH, Colavita A (2011) VANG-1 and PRKL-1 cooperate to negatively regulate neurite formation in *Caenorhabditis elegans*. *PLoS Genet* 7:e1002257. [CrossRef Medline](#)
- Santy LC (2002) Characterization of a fast cycling ADP-ribosylation factor 6 mutant. *J Biol Chem* 277:40185–40188. [CrossRef Medline](#)
- Santy LC, Casanova JE (2001) Activation of ARF6 by ARNO stimulates epithelial cell migration through downstream activation of both Rac1 and phospholipase D. *J Cell Biol* 154:599–610. [CrossRef Medline](#)
- Sato A, Yamamoto H, Sakane H, Koyama H, Kikuchi A (2010) Wnt5a regulates distinct signalling pathways by binding to Frizzled2. *EMBO J* 29:41–54. [CrossRef Medline](#)
- Schmitt AM, Shi J, Wolf AM, Lu CC, King LA, Zou Y (2006) Wnt-Ryk

- signalling mediates medial-lateral retinotectal topographic mapping. *Nature* 439:31–37. [Medline](#)
- Shafer B, Onishi K, Lo C, Colakoglu G, Zou Y (2011) Vangl2 promotes Wnt/planar cell polarity-like signaling by antagonizing Dvl1-mediated feedback inhibition in growth cone guidance. *Dev Cell* 20:177–191. [CrossRef Medline](#)
- Shimizu K, Sato M, Tabata T (2011) The Wnt5/planar cell polarity pathway regulates axonal development of the *Drosophila* mushroom body neuron. *J Neurosci* 31:4944–4954. [CrossRef Medline](#)
- Tissir F, Bar I, Jossin Y, De Backer O, Goffinet AM (2005) Protocadherin Celsr3 is crucial in axonal tract development. *Nat Neurosci* 8:451–457. [Medline](#)
- Wang Y, Nathans J (2007) Tissue/planar cell polarity in vertebrates: new insights and new questions. *Development* 134:647–658. [CrossRef Medline](#)
- Wang Y, Zhang J, Mori S, Nathans J (2006) Axonal growth and guidance defects in Frizzled3 knock-out mice: a comparison of diffusion tensor magnetic resonance imaging, neurofilament staining, and genetically directed cell labeling. *J Neurosci* 26:355–364. [CrossRef Medline](#)
- Wolf AM, Lyuksyutova AI, Fenstermaker AG, Shafer B, Lo CG, Zou Y (2008) Phosphatidylinositol-3-kinase-atypical protein kinase C signaling is required for Wnt attraction and anterior-posterior axon guidance. *J Neurosci* 28:3456–3467. [CrossRef Medline](#)
- Yam PT, Langlois SD, Morin S, and Charron F (2009) Sonic hedgehog guides axons through a noncanonical, Src-family-kinase-dependent signaling pathway. *Neuron* 62:349–362. [CrossRef Medline](#)
- Yamamoto A, Nagano T, Takehara S, Hibi M, Aizawa S (2005) Shisa promotes head formation through the inhibition of receptor protein maturation for the caudalizing factors, Wnt and FGF. *Cell* 120:223–235. [CrossRef Medline](#)
- Yoshikawa S, McKinnon RD, Kokel M, Thomas JB (2003) Wnt-mediated axon guidance via the *Drosophila* Derailed receptor. *Nature* 422:583–588. [CrossRef Medline](#)
- Yu A, Rual JF, Tamai K, Harada Y, Vidal M, He X, Kirchhausen T (2007) Association of Dishevelled with the clathrin AP-2 adaptor is required for Frizzled endocytosis and planar cell polarity signaling. *Dev Cell* 12:129–141. [CrossRef Medline](#)
- Zallen JA (2007) Planar polarity and tissue morphogenesis. *Cell* 129:1051–1063. [CrossRef Medline](#)
- Zhou L, Bar I, Achouri Y, Campbell K, De Backer O, Hebert JM, Jones K, Kessar N, de Rouvoit CL, O’Leary D, Richardson WD, Goffinet AM, Tissir F (2008) Early forebrain wiring: genetic dissection using conditional Celsr3 mutant mice. *Science* 320:946–949. [CrossRef Medline](#)
- Zou Y (2012) Does planar cell polarity signaling steer growth cones? *Curr Top Dev Biol* 101:141–160. [CrossRef Medline](#)
- Zou Y, Stoeckli E, Chen H, Tessier-Lavigne M (2000) Squeezing axons out of the gray matter: a role for slit and semaphorin proteins from midline and ventral spinal cord. *Cell* 102:363–375. [CrossRef Medline](#)